Temperature dependence of the E_{2h} phonon mode of wurtzite GaN/AlN quantum dots

J. A. Budagosky, A. García-Cristóbal, and A. Cros[a)]
Institut de Ciència dels Materials, Universitat de València, E-46071 València, Spain

Raman scattering has been used to study the temperature dependence of the frequency and linewidth of the E_{2h} phonon mode of GaN/AlN quantum dot stacks grown on $6H$-SiC. The evolution of the nonpolar phonon mode was analyzed in the temperature range from 80 to 655 K for both quantum dots and barrier materials. The experimental results are interpreted by comparison with a model that takes into account symmetric phonon decay and the different thermal expansions of the constituents of the heterostructure. We find a small increase in the anharmonic parameters of the phonon modes in the heterostructure with respect to bulk. © *2008 American Institute of Physics.*
[DOI: 10.1063/1.3006892]

I. INTRODUCTION

Systems based on semiconductor self-assembled quantum dots (QDs) have been established to be promising candidates for the development of optoelectronic devices with enhanced efficiency. Up to now, research efforts on these systems have concentrated mainly on the study of the emission properties of the dots.[1] Despite the importance of phonon dynamics in device engineering,[2] basic phonon properties, such as the temperature dependence of phonon frequencies and linewidths, have been addressed only for few nanostructured materials.[3–7] Among III–V semiconductors, group III nitrides excel for their outstanding thermal and chemical stability, essential for high-temperature and high-power devices.[8,9] The determination of the temperature dependence of the vibrational modes of GaN/AlN QDs would allow the use of Raman scattering as an *in situ* space and time resolved temperature diagnostic tool[10] for QD based devices.

The temperature dependence of phonons in semiconductors is interpreted in terms of anharmonic processes[11] and thermal expansion effects.[12] A temperature increase results in an increase in the phonon scattering rate and a decrease in the phonon lifetimes, with a consequent increase in the Raman linewidths. In addition to its dependence on phonon coupling, the expansion of the material that results from heating also changes the phonon frequency. Concerning the E_{2h} phonon mode, anharmonic effects in AlN are dominated by two-phonon decay channels.[13] In bulk GaN, due to the large frequency gap between the E_{2h} mode and the acoustic branches, three-phonon decay channels dominate.[14] Besides depending on the details of phonon dispersion, the interaction among optical phonons may be influenced by the presence of interfaces and confinement effects. In this respect, investigations performed on Si nanocrystals of various sizes indicated an increase in the value of the phonon decay anharmonic parameters as the crystal size was decreased.[15] This interesting effect, ascribed to increasing phonon-

interface scattering, has important implications in the process of self-heating of optoelectronic devices based on nanostructures.[16]

In this paper we report on Raman scattering studies on the temperature response of the E_{2h} phonon in GaN QDs and the AlN spacer surrounding the dots. A wide temperature range, covering from 80 to 655 K, has been analyzed. The experimental results have been interpreted by a model taking into account three main processes: the intrinsic thermal expansion of the crystal lattice, the symmetric decay of E_{2h} phonons into two and three acoustic phonons of lower energies, and the thermal strain induced by the different expansion coefficients of the constituents of the heterostructure. We will discuss the relative importance of these effects on the observed phonon energies and linewidths as a function of temperature.

II. SAMPLE AND EXPERIMENTAL DETAILS

Micro-Raman measurements were performed in backscattering configuration [$z(x,x)\bar{z}$ geometry] with a Jobin-Yvon T64000 Raman spectrometer equipped with a confocal microscope. The 514.5 nm line of an Ar$^+$ laser was used as excitation source. The scattered light was filtered through a holographic Notch filter in order to eliminate the elastically dispersed light. To focus the laser light on the sample and collect the signal to the spectrometer, a $10\times$ objective was used. The spectrometer was calibrated carefully using the laser line and a silicon sample as a reference. The spectral resolution was set to 0.2 cm^{-1}. A standard microscope Konti-Cryostat, from Cryovac, was used to cover the temperature range from 80 to 300 K. Above room temperature, the sample was heated in a Linkam-TS1500 heating stage.

The sample studied was grown on a $6H$-SiC (0001) substrate in a MECA2000 plasma-assisted molecular beam epitaxy chamber at a temperature of 730 °C. Active nitrogen was supplied by a radio-frequency plasma cell. GaN QDs were synthesized using the modified Stranski–Krastanov growth mode.[17] The sample consists of stacks of 200 planes of GaN QDs separated by 8 nm thick AlN barriers. The nominal amount of GaN deposited in each period is equiva-

---

lent to 6 monolayers (MLs). From these, 2 MLs form the wetting layers on top of which GaN QDs grow. The last period was left uncapped for atomic force microscopy (AFM) characterization. Details of the growth and structural characterization of the sample have been reported elsewhere.[18] The mean QD height and diameter, as determined from AFM measurements, were 4 and 50 nm, respectively, with areal density of 4.5×10^{10} dots/cm^2.

III. THEORY

The temperature dependence of the phonon frequency and linewidth can be obtained from the anharmonic terms of the vibrational Hamiltonian of the crystal lattice.[19] This anharmonicity is responsible for the thermal expansion of the lattice and the phonon-phonon interaction. Considering symmetric decay channels, the variation in the linewidth with temperature can be expressed as[20]

$$\Gamma(T) = \Gamma_0 + A[1 + 2\eta(T, \omega_0/2)] + B[1 + 3\eta(T, \omega_0/3) + 3\eta^2(T, \omega_0/2)], \qquad (1)$$

where ω_0 is the phonon frequency at 0 K, $\eta(T, \omega) = [\exp(\hbar\omega/K_B T) - 1]^{-1}$ is the Bose–Einstein distribution function, and A and B are constant factors describing the probability of the two and three phonon decay processes, respectively. The term Γ_0 is temperature independent and represents an intrinsic damping due to disorder, strain fluctuations, or confining effects.[21–23] Attention should be given to the fact that Γ_0 is not the value of the linewidth at 0 K but $\Gamma_0 + A + B$.

Concerning the phonon frequency, we will consider three different sources for its variation with temperature relative to the frequency Ω_0 in the perfect (strained) harmonic lattice:[24]

$$\omega(T) = \Omega_0 + \Delta\omega_e(T) + \Delta\omega_d(T) + \Delta\omega_s(T). \qquad (2)$$

The term $\Delta\omega_e(T)$ represents the shift due to the thermal expansion characteristic of the lattice in the bulk material and depends on the thermal expansion coefficients parallel (α_c) and perpendicular (α_a) to the wurtzite c axis. In the isotropic approximation, this term can be written as[24]

$$\Delta\omega_e(T) = \Omega_0\left\{e^{-\gamma\int_0^T[\alpha_c(T') + 2\alpha_a(T')]dT'} - 1\right\}. \qquad (3)$$

The Grüneisen parameter γ takes the values 1.50 for GaN (Ref. [25]) and 1.34 for AlN.[26] These values are the same adopted in Refs. [13] and [14] and will allow the comparison of our system with the bulk results therein reported. The second term $\Delta\omega_d(T)$ incorporates the contribution to the phonon frequency shift due to the decay of zone-center optical phonons into phonons of lower energy. We have considered as most important decay channels those corresponding to a decay into two and three identical phonons (symmetric decay).[11]

$$\Delta\omega_d(T) = C[1 + 2\eta(T, \omega_0/2)] + D[1 + 3\eta(T, \omega_0/3) + 3\eta^2(T, \omega_0/3)], \qquad (4)$$

where C and D are anharmonic constants for the decay of one phonon into two or three equal phonons (i.e., processes involving three and four phonons). They give a measure of

the probability of occurrence of each process. Notice that Ω_0 and ω_0 are not independent constants but are related through the anharmonic parameters C and D: $\omega_0 = \Omega_0 + C + D$.

The third term $\Delta\omega_s(T)$ is the contribution to the Raman shift due to strain arising from the different thermal expansion coefficients of the materials that constitute the heterostructure, namely, GaN, AlN, and SiC.[27,28] Due to the fact that the GaN and AlN contents of the QD sample are very different, the dependence of this "thermal strain" with temperature will be analyzed separately for both materials in the following sections.

A. AlN spacer thermal strain

Two sources should be considered to evaluate the thermal strain in the AlN spacer: the influence of the GaN QDs and the 6H-SiC substrate. Since the amount of AlN in the samples represents 85% of the material in the heterostructure, we will neglect the thermal influence of the GaN QDs. Concerning the substrate, the temperature dependent in-plane strain induced in the spacer by its different expansion coefficients can be written as[24]

$$\varepsilon_{xx}^{\text{AlN/SiC}}(T) = \frac{a^{\text{AlN/SiC}}(T) - a_0^{\text{AlN}}(T)}{a_0^{\text{AlN}}(T)}$$
$$= (1 + \varepsilon_g)\frac{1 + \int_{Tg}^T \alpha_a^{\text{SiC}}(T')dT'}{1 + \int_{Tg}^T \alpha_a^{\text{AlN}}(T')dT'} - 1, \qquad (5)$$

where ε_g is the residual strain in the spacer at the growth temperature $T_g = 1003$ K, α_a^{SiC} and α_a^{AlN} are the in-plane expansion coefficients of bulk 6H-SiC and AlN, $a_0^{\text{AlN}}(T)$ is the bulk AlN lattice parameter, and $a^{\text{AlN/SiC}}(T)$ is that modified by the thermal mismatch of the substrate. ε_g is found to be very small and has been neglected in the calculations.

The biaxial strain approximation allows the determination of the corresponding axial thermal strain through the elastic constants of AlN (Ref. [29]) C_{13} and C_{33},

$$\varepsilon_{zz}^{\text{AlN/SiC}}(T) = \frac{c^{\text{AlN/SiC}}(T) - c_0^{\text{AlN}}(T)}{c_0^{\text{AlN}}(T)} = -\frac{2C_{13}}{C_{33}}\varepsilon_{xx}^{\text{AlN/SiC}}(T). \qquad (6)$$

Finally, we can relate the thermal strain with the phonon shift through the phonon deformation potential approximation,

$$\Delta\omega_s^{\text{AlN/SiC}}(T) = 2\left(a_{\text{AlN}} - b_{\text{AlN}}\frac{C_{13}}{C_{33}}\right)\varepsilon_{xx}^{\text{AlN/SiC}}(T), \qquad (7)$$

a_{AlN} and b_{AlN} being the E_{2h} phonon deformation potentials of AlN.[30]

B. GaN QDs thermal strain

Similarly as in Eq. (7), in terms of the GaN deformation potentials[31] the frequency shift due to the thermal strain will take the form
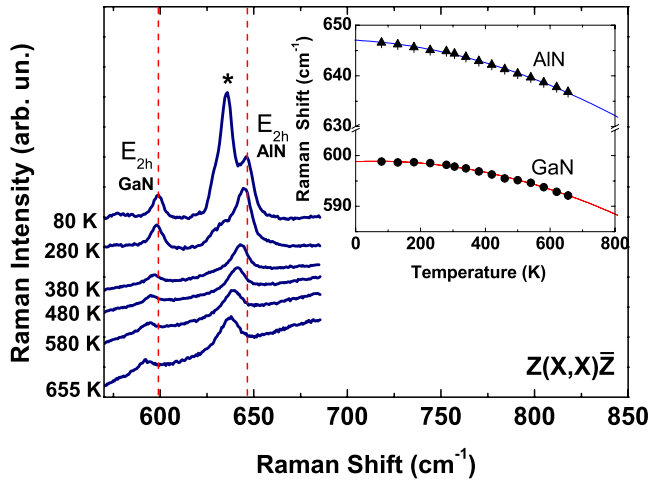
FIG. 1. (Color online) Micro-Raman spectra recorded at various temperatures under $z(x,x)\bar{z}$ backscattering geometry. The inset represents the temperature-dependent Raman shifts of the E_{2h} mode of the AlN spacer (triangles) and the GaN QDs (dots). The lines are second order polynomial fits to the experimental points.

$$\Delta\omega_s^{\text{GaN/AlN}}(T) = 2a_{\text{GaN}}\varepsilon_{xx}^{\text{GaN/AlN}}(T) + b_{\text{GaN}}\varepsilon_{zz}^{\text{GaN/AlN}}(T). \quad (8)$$

The main thermal influence on the QDs will arise from the different thermal expansion coefficients of the spacer. Several peculiarities arise in the determination of $\varepsilon_{xx}^{\text{GaN/AlN}}(T)$ and $\varepsilon_{zz}^{\text{GaN/AlN}}(T)$ when compared with Sec. III A. First, the AlN spacer is modified by the thermal properties of the SiC matrix. This effect has been taken into account considering for the spacer the lattice parameters $a^{\text{AlN/SiC}}(T)$ and $c^{\text{AlN/SiC}}(T)$ obtained from Eqs. (5) and (6). Additionally, it is well known that the biaxial approximation is not fulfilled in stacks of QDs, even for dots with aspect ratio (height/diameter) smaller than 0.1.[32] To determine the in-plane and axial thermal strain in the dots, we have modeled the strain distribution in an array of lattice-mismatched GaN/AlN QDs. The calculations have been performed in the framework of the elastic continuum theory by using the inclusion method of Eshelby.[33] The model considers the dot as a misfitting inclusion in an AlN matrix modified, as indicated before, by the SiC substrate. The geometry adopted for the dot is based on AFM and transmission electron microscopy characterizations. Each dot is represented by a truncated cone with 4 nm height and a diameter of 50 nm. For each temperature, the values of the lattice parameters $a^{\text{AlN/SiC}}(T)$ and $c^{\text{AlN/SiC}}(T)$ of the AlN matrix are taken as input to the model, together with the lattice parameters of bulk GaN (Ref. 28) $[a_0^{\text{GaN}}(T)$ and $c_0^{\text{GaN}}(T)]$. The strain tensor components $\widetilde{\varepsilon}_{xx}^{\text{GaN/AlN}}(T)$ and $\widetilde{\varepsilon}_{zz}^{\text{GaN/AlN}}(T)$ calculated at the center of the dot are taken as representatives of the whole dot. To determine the thermal strain at a given temperature, the values of strain at the growth temperature T_g are subtracted from the results,

$$\varepsilon_{xx}^{\text{GaN/AlN}}(T) = \widetilde{\varepsilon}_{xx}^{\text{GaN/AlN}}(T) - \widetilde{\varepsilon}_{xx}^{\text{GaN/AlN}}(T_g),$$

$$\varepsilon_{zz}^{\text{GaN/AlN}}(T) = \widetilde{\varepsilon}_{zz}^{\text{GaN/AlN}}(T) - \widetilde{\varepsilon}_{zz}^{\text{GaN/AlN}}(T_g). \quad (9)$$
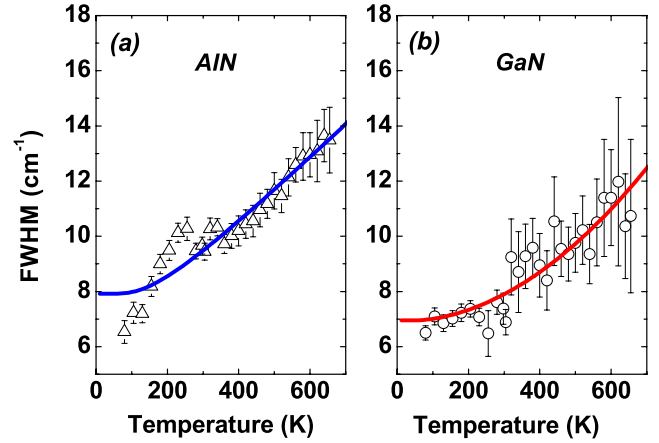

FIG. 2. (Color online) Linewidths of the E_{2h} phonon mode of (a) the AlN spacer and (b) the GaN QDs. The full lines correspond to a fit to the data using Eq. (1).

IV. RESULTS AND DISCUSSION

Representative spectra of the QD sample recorded at various temperatures are shown in Fig. 1. The active Raman modes of wurtzite GaN and AlN in the $z(x,x)\bar{z}$ configuration are E_{2h} and $A_1(LO)$. However, in our experiment the $A_1(LO)$ mode was too weak to be detected. Three peaks can be observed in the frequency range shown in the spectra. The E_{2h} mode characteristic of the GaN QDs appears around 600 cm^{-1}, while that of the AlN spacer is found at higher frequency, around 650 cm^{-1}. The peak labeled with an asterisk corresponds to the SiC substrate, and its intensity decreases rapidly with the increasing temperature. The Raman peaks exhibit a progressive broadening and shift to lower energies as the temperature is raised from 80 to 655 K.

We will first turn our attention to the evolution of the linewidth (FWHM) of the E_{2h} mode with temperature. Figures 2(a) and 2(b) show the experimental results obtained for the spacer and the QDs, together with the fitting by means of Eq. (1). The parameters used have been collected in Table I. As expected from the anharmonic theory, the phonon linewidths increase with temperature. Their values are found to be much larger than in bulk ($\approx$2 and 4 cm^{-1} for GaN and AlN, respectively[13,14]), a characteristic that can be ascribed to the inhomogeneous strain distribution in the heterostructures and the scattering of the phonons by the interfaces. In any case, at room temperature the FWHM is comparable to that found for similar GaN/AlN QD samples[32] and AlN films grown on sapphire.[24] Our analysis indicates that the two-

TABLE I. Fitting parameters of the phonon linewidths of AlN and GaN obtained using Eq. (1). The corresponding bulk values are given for comparison.

Material	Γ_0 (cm^{-1})	A (cm^{-1})	B (cm^{-1})
AlN (spacer)	5.02	2.90	0.00
AlN (bulk[a])	0.70	2.12	0.00
GaN (QDs)	6.70	0.00	0.27
GaN (bulk[b])	1.4	0.00	0.10

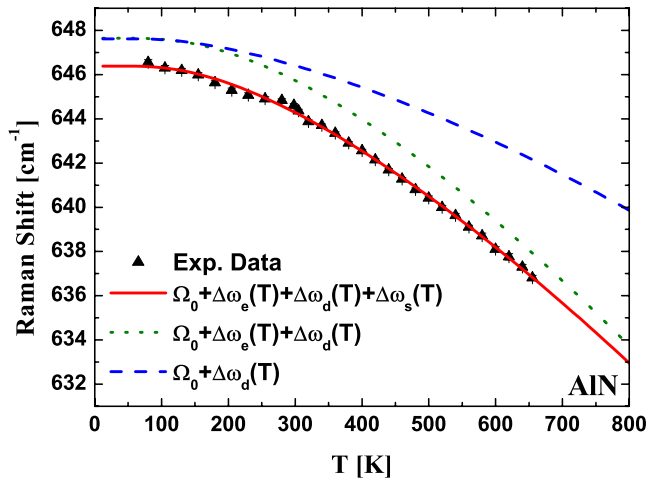[a]Reference 13.
[b]Reference 14.

FIG. 3. (Color online) Shift in E_{2h} Raman mode of the AlN spacer as a function of temperature. The full line is a fit using Eq. (2). The dotted line includes the influence of phonon decay and thermal expansion, while the dashed line represents the contribution of phonon decay.
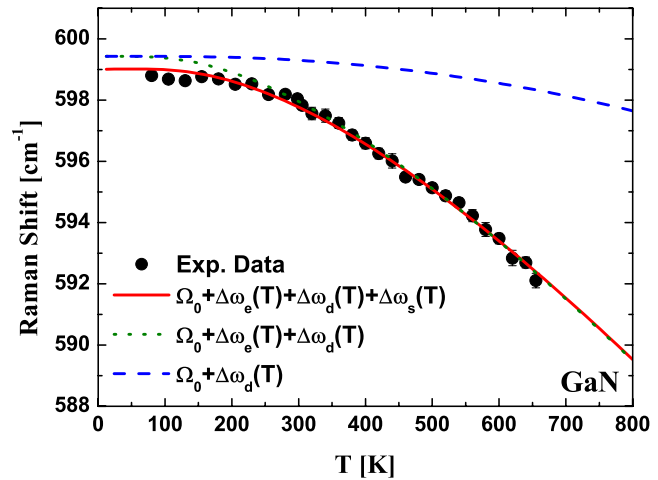

FIG. 4. (Color online) Shift in E_{2h} Raman mode of GaN QDs as a function of temperature. The full line is a fit using Eq. (2). The dotted line includes the influence of phonon decay and thermal expansion, while the dashed line represents the contribution of phonon decay.

phonon decay is the dominant mechanism involved in the increase in the E_{2h} phonon linewidth of the AlN spacer. On the other hand, similar as in bulk,[14] for the GaN QDs the evolution of the phonon width with temperature is better explained considering a symmetric three phonon decay channel. A comparison of the anharmonic A and B parameters of our sample with those of bulk[13,14] (see Table I) indicates an increase in their values by a factor of 2.7 for the GaN QDs and only 1.4 for the AlN spacer. This difference could be due to the larger confinement effects expected in QDs than in the two-dimensional spacer. This increase is comparable to that reported for nanocrystalline silicon samples of similar size.[15] Besides the anharmonic effects discussed concerning the linewidth, the phonon frequency is strongly influenced by the intrinsic thermal properties of the material and, in heterostructures, by the mismatch between the thermal expansion coefficients of the different constituents.

In Fig. 3 we have plotted the evolution of the frequency of the E_{2h} phonon mode of the AlN spacer with temperature, together with the result of Eq. (2) (full line). The values of the three fitting parameters used in the calculations are plotted in Table II, together with the corresponding bulk values.[13] The frequency of the phonon mode is redshifted more than 13 cm^{-1} with respect to the bulk value, an indication of the mean tensile strain of the material. The values of the anharmonic parameters indicate that, similar as in

bulk, two phonon decay processes prevail over three phonon ones. However, in our heterostructure this last contribution cannot be neglected. The influence of the thermal strain ($\Delta\omega_s$) can be grasped by looking at the dotted line, where this contribution has been subtracted. It results in the overestimation of the experimental data by 1.25 cm^{-1} at low temperature, with a change in the curvature of the line that is more important at higher energies. The dashed line represents the contribution due to phonon decay ($\Delta\omega_d$), which is found to be of similar magnitude than the intrinsic thermal expansion ($\Delta\omega_e$). More recent evaluations of the AlN Grüneisen parameter[34,35] than the one considered here[26] increase its value up to 1.71. As a consequence, the influence of the AlN thermal expansion will be enhanced, decreasing the relative importance of the phonon decay in the temperature evolution of the Raman shift. A fit of our experimental data with $\gamma=1.71$ (Ref. 35) gives for the AlN anharmonic parameters values of $C=-1.63$ cm^{-1} and $D=-0.14$ cm^{-1}, with a decrease in their absolute value with respect to those reported in Table II. It should be noticed that, although in our system the contribution of the thermal strain is much weaker than that of the intrinsic thermal expansion and two-phonon decay, all three contributions are necessary to explain the experimental data in the measured temperature range.

The result of the fit for the E_{2h} mode of the GaN QDs is shown in Fig. 4 (full line). The corresponding fitting parameters can be found in Table II. The blueshift of the frequency of the mode is larger than 30 cm^{-1} when compared to bulk values and accounts for the large compressive strain of the dots.[36] Similar as in bulk, the contribution due to two phonon decay channels can be neglected in the QD. Besides, the three phonon decay contribution (dashed line) is almost flat so that the intrinsic thermal expansion ($\Delta\omega_e$) dominates the temperature evolution of the phonon frequency. The value of the anharmonic parameter D is slightly larger than that of bulk GaN, although the increase is not as significant as in the FWHM (see Table I). Despite being completely surrounded by AlN, the thermal influence of the spacer on the dots is very small. In the dotted line the contribution of the thermal

TABLE II. Parameters used to fit the E_{2h} Raman mode dependence on temperature in Figs. 3 and 4 with Eq. (2). The bulk values are included as references.

Material	ω_0 (cm^{-1})	C (cm^{-1})	D (cm^{-1})
AlN (spacer)	647.62	−1.88	−0.23
AlN (bulk[a])	661.1	−2.37	0.00
GaN (spacer)	599.43	0.00	−0.11
GaN (bulk[b])	569.10	0.00	−0.09

[a]Reference 13.
[b]Reference 14.

strain has been subtracted from the total frequency. Its influence is only important at low temperatures, with a value of only 0.4 cm^{-1}.

V. CONCLUSION

In conclusion, we have studied the temperature dependence of the E_{2h} Raman mode of stacks of GaN/AlN QDs in the range from 80 to 655 K. We found that symmetric two phonon decay in the AlN spacer and three phonon decay in the GaN QDs are the most important anharmonic mechanisms governing the decay of the E_{2h} phonon mode. Changes in temperature due to the intrinsic thermal strain dominate for GaN, and their contribution is comparable to that of the anharmonic mechanisms for AlN. We found that it is necessary to take into account the different thermal expansion coefficients of the constituents of the heterostructure to understand the experimental data. The fit of the experimental points (FWHM and the phonon frequency) indicates a small increase in the value of the anharmonic parameters with respect to bulk. This increase may be related to size effects but should be further investigated for heterostructures of different sizes. Finally, we would like to point out that the dependence of the phonon mode with temperature can be easily fitted by a second order polynomial function (see inset of Fig. 1) and may allow to use the Raman scattering to monitor the working temperature of optical devices implemented with GaN QDs.

ACKNOWLEDGMENTS

[1] D. Bimberg, M. Grundmann, and N. N. Ledentsov, *Quantum Dots Heterostructures* (Wiley, Chichester, 1999).
[2] M. A. Stroscio and M. Dutta, *Phonons in Nanostructures* (Cambridge University Press, Cambridge, 2001).
[3] J. Niu, J. Sha, and D. Yang, Scr. Mater. **55**, 183 (2006).
[4] X. B. Chen, J. Huso, J. L. Morrison, L. Bergman, and A. P. Purdy, J. Appl. Phys. **98**, 026106 (2005).
[5] H. D. Li, K. T. Yue, Z. L. Lian, S. L. Zhang, L. X. Zhou, S. L. Zhang, Z. J. Shi, Z. N. Gu, B. B. Liu, R. S. Yang, H. B. Yang, G. T. Zou, Y. Zhang, and S. Iijima, Appl. Phys. Lett. **76**, 2053 (2000).
[6] K. A. Alim, V. A. Fonoberov, M. Shamsa, and A. A. Balandin, J. Appl. Phys. **97**, 124313 (2005).
[7] K. Edamatsu, T. Itoh, K. Matsuda, and S. Saikan, Phys. Rev. B **64**, 195317 (2001).
[8] S. Nakamura, S. Pearton, and G. Fasol, *The Blue Laser Diode* (Springer, Berlin, 2000).
[9] J. I. Pankove and T. D. Moustakas, *Gallium Nitrides I*, Semiconductors and Semimetals, Vol. 50 (Academic, SanDiego, CA, 1998).
[10] M. Kuball, J. M. Hayes, M. J. Uren, I. Martin, J. C. H. Birbeck, R. S. Balmer, and B. T. Hughes, IEEE Electron Device Lett. **23**, 7 (2002).
[11] M. Balkanski, R. F. Wallis, and E. Haro, Phys. Rev. B **28**, 1928 (1983).
[12] T. Inoue, Y. Toda, K. Hoshino, T. Someya, and Y. Arakawa, Phys. Status Solidi C **0**, 2428 (2003).
[13] D. Y. Song, M. Holtz, A. Chandolu, S. A. Nikishin, E. N. Mokhov, Yu. Makarov, and H. Helava, Appl. Phys. Lett. **89**, 021901 (2006).
[14] D. Y. Song, M. Basavaraj, S. A. Nikishin, M. Holtz, V. Soukhoveev, A. Usikov, and V. Dmitriev, J. Appl. Phys. **100**, 113504 (2006).
[15] P. Mishra and K. P. Jain, Phys. Rev. B **62**, 14790 (2000).
[16] A. Khitun, A. Balandin, J. L. Liu, and K. L. Wang, J. Appl. Phys. **88**, 696 (2000).
[17] N. Gogneau, D. Jalabert, E. Monroy, T. Shibata, M. Tanaka, and B. Daudin, J. Appl. Phys. **94**, 2254 (2003).
[18] N. Gogneau, F. Fossard, E. Monroy, S. Monnoye, H. Mank, and B. Daudin, Appl. Phys. Lett. **84**, 4224 (2004).
[19] J. Menéndez and M. Cardona, Phys. Rev. B **29**, 2051 (1984).
[20] P. G. Klemens, Phys. Rev. **148**, 845 (1966).
[21] H. H. Burke and I. P. Herman, Phys. Rev. B **48**, 15016 (1993).
[22] H. Richter, Z. P. Wang, and L. Ley, Solid State Commun. **39**, 625 (1981).
[23] L. A. Falkovsky, J. M. Bluet, and J. Camassel, Phys. Rev. B **55**, R14697 (1997).
[24] A. Link, K. Bitzer, W. Limmer, R. Sauer, C. Kirchner, V. Schwegler, M. Kamp, D. G. Ebling, and K. W. Benz, J. Appl. Phys. **86**, 6256 (1999).
[25] H. Siegle, A. R. Goñi, C. Thomsen, C. Ulrich, K. Siassen, and D. J. As D. Chikora, Proceedings of the MRS Spring Meeting, San Francisco, 1997 (unpublished).
[26] P. Perlin, A. Polian, and T. Suski, Phys. Rev. B **47**, 2874 (1993).
[27] K. Wang and R. R. Reeber, Mater. Res. Soc. Symp. Proc. **482**, 867 (1998).
[28] R. R. Reeber and K. Wang, J. Mater. Res. **15**, 40 (1999).
[29] I. Vurgaftman and J. R. Meyer, J. Appl. Phys. **94**, 3675 (2003).
[30] J. Gleize, M. A. Renucci, J. Frandon, E. Bellet-Amalric, and B. Daudin, J. Appl. Phys. **93**, 2065 (2003).
[31] V. Yu. Davydov, N. S. Averkiev, I. N. Goncharuk, D. K. Nelson, I. P. Nikitina, A. S. Polkovnikov, A. N. Smirnov, M. A. Jacobson, and O. K. Semchinova, J. Appl. Phys. **82**, 5097 (1997).
[32] A. Cros, N. Garro, J. M. Llorens, A. García-Cristóbal, A. Cantarero, N. Gogneau, E. Monroy, and B. Daudin, Phys. Rev. B **73**, 115313 (2006).
[33] J. D. Eshelby, Proc. R. Soc. London **241**, 376 (1957).
[34] A. R. Goñi, H. Siegle, K. Syassen, C. Thomsen, and J. M. Wagner, Phys. Rev. B **64**, 035205 (2001).
[35] M. Kuball, J. M. Hayes, A. D. Prins, N. W. A. van Uden, D. J. Dunstan, Y. Shi, and J. H. Edgar, Appl. Phys. Lett. **78**, 724 (2001).
[36] J. Gleize, J. Frandon, F. Demangeot, M. A. Renucci, C. Adelmann, B. Daudin, G. Feuillet, B. Damilano, N. Grandjean, and J. Massies, Appl. Phys. Lett. **77**, 2174 (2000).